JOURNAL OF Materials CHEMISTRY

Semiconducting $CuCl_xBr_{1-x}$ ($x = 0$–1) nanocrystals in thin films: synthesis and characterization

Ganesh Suyal,*† Martin Mennig and Helmut Schmidt

Institüt für Neue Materialien, D-66125 Saarbrücken, Germany

Received 15th April 2002, Accepted 26th July 2002
First published as an Advance Article on the web 21st August 2002

Thin films containing semiconducting nanocrystals of $CuCl_xBr_{1-x}$ ($x = 0$–1) were synthesized by the sol–gel process, by stepwise substitution of chloride ions by bromide ions. Cuprous oxide was used as the precursor for copper, HCl and HBr as halide sources, and the matrix sol was synthesized from 3-glycidoxypropyl-(trimethoxy)silane (GPTS) and tetraethoxysilane (TEOS). The films were characterized using ultraviolet–visible (UV-VIS) spectroscopy, high-resolution transmission electron microscopy (HR-TEM) and X-ray diffraction analysis. Thin films (thickness 0.7–1.0 μm) containing cubic $CuCl_xBr_{1-x}$ ($x = 1$–0) nanoparticles were obtained. For the samples having no bromide, the absorption spectrum showed a sharp absorption edge at 371 nm. Addition of HBr shifted the peak towards a higher wavelength, giving a peak that is characteristic of $CuCl_xBr_{1-x}$; the addition of 1.85×10^{-2} mole of HBr leads to the complete substitution of chloride by bromide ions. The same observations were also made using X-ray diffraction.

Introduction

Thin films doped with semiconductor microcrystals have drawn significant scientific attention due to their non-linear optical properties.[1,2] A lot of research has been conducted since Jain and Lind[3] first observed high optical non-linearity in CdS_xSe_{1-x} doped glasses. However most of these studies have been limited to materials like CdS_xSe_{1-x}, CdTe, GaAs and CdS, with very low concentrations of microcrystals. These compounds show third order non-linearity. Two quantum confinement regimes may be considered as the origin of the non-linear enhancement of semiconductors in glasses, depending on the ratio of the radius R of the microcrystal and the exciton Bohr radius.[4,5]

In the case of strong confinement where the microcrystal size is smaller than the Bohr radius, both electron and hole confinements were assumed to be dominant relative to the coulomb interaction.[6] This results in a splitting of both the valence and conduction band into a series of sub-bands. In the weak confinement case, which corresponds to the radius R being larger than the Bohr radius, the coulomb interaction is retained and the exciton is confined. In this case discrete sub-bands of excitons with lower energies are formed. Glasses containing copper halide nanoparticles are included in the second category.

Non-linear properties of semiconducting nanocrystals have been studied by various authors.[7–9] Copper halide containing glasses have been reported to show non-linear suceptibilitiy $\chi^{(3)}$ of the order of 10^{-9}–10^{-8} esu,[10] which is still insufficient for the realization of practical devices.[11] Though these glasses are mainly being studied for their third order nonlinear properties, they can also find applications as optical filters (UV-filters) due to their sharp absorption edge at the transition wavelength between ultraviolet and visible regions.

Semiconductor nanocrystals containing such filter glasses with a sharp absorption edge are commercially available and produced by Corning[12] and Schott[13] by the melting method, which, being a high temperature process, makes these filters costly and thus limits their applicability. The investigation of a sol–gel as a new and cheaper alternative for coating glass substrates has also proceeded at a rapid pace over the last few years. Sol–gel can be an especially suitable alternative to synthesize thin films containing copper halide nanoparticles. However the low temperatures used in sol–gel synthesis and the H_2O content in the gel shift the Cu^{2+}–Cu^{+} equilibrium mainly to Cu^{2+} thus making it difficult to prepare films exclusively containing monovalent copper. The aim of this work is the synthesis and characterization of glass films containing semiconducting nanocrystals of copper halides using the sol–gel route.

It has been shown elsewhere,[14] that thin films containing CuCl and CuBr nanoparticles have sharp absorption edges at 371 and 411 nm respectively. In order to find application as an optical filter, which completely blocks the UV radiation from the visible light, the absorption peak has to be shifted to 400 nm. Therefore the synthesis of thin films containing $CuCl_xBr_{1-x}$ ($x = 0$–1) particles has been carried out in the present work.

Experimental

To synthesize thin films containing $CuCl_xBr_{1-x}$ ($x = 1$–0) nanoparticles, 0.60 g of cuprous oxide was mixed with 7.5 ml of acetonitrile using an ultrasonic bath for 15 min, and then 17.5 ml of 3-glycidoxypropyl(trimethoxy)silane (GPTS)–tetraethoxysilane (TEOS) sol (synthesized as in ref. 14) was added to it. After stirring at 25 °C for 15 min, 3.0 g of hydrochloric acid (37%) was added dropwise to get a clear and transparent sol. The resulting sol was stirred for 48 h at 25 °C and 0.45 g hydrobromic acid (40%) was added. Sodalime and fused silica glass substrates were dip-coated at a withdrawing speed of 4 mm s^{-1}. A further 0.45 g hydrobromic acid was added to the sol and the substrates were dip-coated again. This process was repeated several times. Samples were dried in an oven at 60 °C for 15 min and the coatings were cured in air by passing the samples through the UV-IR beltron machine (1200 W, 150 °C). The flow diagram representing the synthesis of thin films containing $CuCl_xBr_{1-x}$ ($x = 1$–0) nanoparticles is shown in Fig. 1.

To investigate the optical properties, UV-VIS absorption spectra of the films coated on the glass slides were recorded with an OMEGA 30 UV-VIS spectrophotometer (Bruins Instrument). Low temperature UV-VIS measurements were

†Present address: Federal Institute of Technology, IMX-LC, Ecublens, 1015 Lausanne, Switzerland. E-mail: ganesh.suyal@epfl.ch

 DOI: 10.1039/b203654c

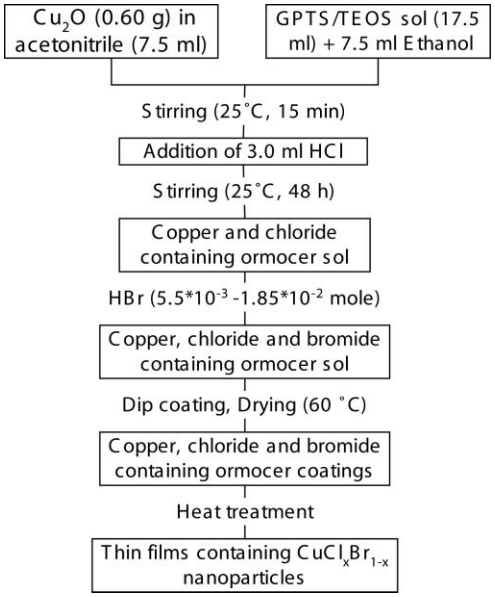

Fig. 1 Flow diagram representing the synthesis of thin films containing $CuCl_xBr_{1-x}$ (x = 1–0) nanoparticles.

carried out on a VARIAN CARY 5E spectrophotometer. Extinction spectra of thin films were recorded at liquid nitrogen temperature (T = 84 K) and at a pressure of 5×10^{-4} mbar. The UV-VIS spectra were recorded at wavelengths ranging from 300 to 1000 nm. Film thickness was measured with a profilometer (diamond stylus, nanosurf).

To obtain information about the crystalline phase of the copper halide nanocrystals, X-ray diffraction measurements were conducted on a Siemens automated diffractometer working at 40 KV and 35 mA with a LiF monochromator and the radiation used was Cu-Kα (1.5405 Å). The diffracted X-rays were collected by scanning between 2θ = 20–60° in 0.04° steps. A JEOL 200 CX high-resolution transmission electron microscope (HR-TEM) was used to perform the electron microscopic characterization of the copper halide nanocrystals in the films. The samples were prepared by scratching off the layer splinters from the copper halide containing coatings. This scratched material was deposited onto a carbon coated copper grid and was investigated using HR-TEM.

Results and discussion

Copper(I) compounds are known to be soluble in only strong acids or strong bases. Hence the chlorination of copper ions was done by incorporating HCl into the sol containing copper oxide. The addition of halide ions greatly increases the solubility of the cuprous salt due to the formation of halocuprate(I) anions[15] of the type CuX_2^- and CuX_3^{2-}, resulting in a green colored transparent solution. Therefore, a suspension of cuprous oxide in acetonitrile was mixed with the matrix sol and the chloride ions were added to obtain a clear solution. Since the stability of the cuprous ions relative to that of the cupric ions may be affected by the solvent, acetonitrile, in which Cu^+ is more stable than Cu^{2+},[16] was chosen as the solvent. In order to obtain $CuCl_xBr_{1-x}$ nanoparticles in thin films, HBr was added stepwise to the solution of Cu_2O in HCl.

Colorless transparent coatings with thicknesses of 0.7–1.0 μm were obtained by a single deposition process after heat treatment in a UV-IR beltron machine connected to a low pressure Hg–Xe lamp (1200 W) and thermal irradiation (150 °C).

The absorption spectra of thin films containing $CuCl_xBr_{1-x}$ nanocrystals were recorded after each addition of HBr to follow the sequential substitution of chloride by bromide ions. The UV-VIS spectra of the samples treated with UV-IR radiation for 4 min, recorded at room temperature after the stepwise addition of hydrobromic acid, are shown in Fig. 2.

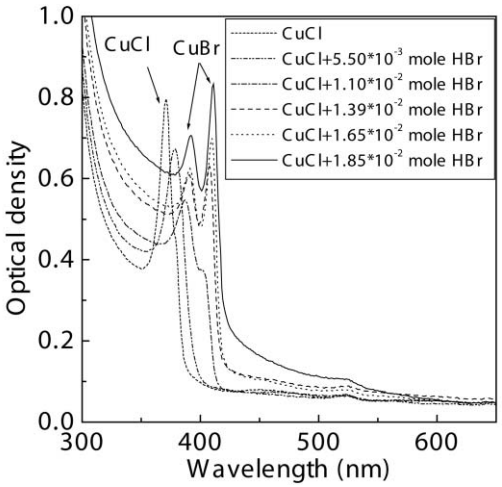

Fig. 2 The UV-VIS absorption spectra of the samples as a function of the molar fraction of HBr (heat treatment at 150 °C in a UV-IR beltron machine, 1200 W for 4 min).

From this figure it is clear that the addition of 5.5×10^{-3} mole HBr shifts the absorption peak slightly towards higher wavelengths but it remains as a single absorption peak, whereas the addition of 1.1×10^{-2} mole HBr shifts the peak towards still higher wavelengths and the single absorption peak splits into two sharp peaks. This absorption spectrum is in good agreement with the $CuCl_xBr_{1-x}$ doped bulk glasses reported by Ruller *et al.*[17] The addition of 1.85×10^{-2} mole HBr changes the absorption spectra significantly and such a sample showed two sharp peaks at 390 and 410 nm, as seen previously in the case of thin films containing CuBr nanocrystals.[14] Thus complete replacement of chloride by bromide ions seems to be taking place in this sample.

In all the spectra shown in Fig. 2, a very weak peak at around 525 nm is also visible. This peak may be assigned to the $^2B_{1g} \rightarrow {}^2A_{1g}$ transition of copper(II) ions in a square-planar coordination.[18]

The substitution of chloride by bromide ions in films can be explained by the fact that the bromide, being less electronegative, would easily replace the chloride in the solution. Since the stability sequence of halide complexes of Cu^+ is known to be I > Br > Cl > F,[19] CuBr is expected to be more stable than CuCl. From this experiment it can be concluded that 1.85×10^{-2} mole HBr per 4.2×10^{-3} mole Cu_2O dissolved in 8.2×10^{-2} mole HCl replaces chloride completely to give a CuBr containing thin film. Therefore the mole fractions of bromine in films were calculated by assuming that the addition of a fraction of this amount of HBr results in the formation of the corresponding fraction of CuBr.

It was observed that after storage of the copper halide samples in air a decrease in the intensity of the characteristic copper halide UV-VIS absorption peak was observed, which vanishes completely after a certain period of time. The possible explanation for this behavior is the very unstable nature of Cu^+. In the presence of moisture and air Cu^+ is known to be oxidized and hydrolyzed to a green product that approaches to Cu^{2+}. It has also been proven experimentally elsewhere.[14]

Absorption spectra of CuCl and CuBr: a comparison

The UV-VIS absorption spectra of thin films containing only CuCl and CuBr and the coatings of the reference sol are shown in Fig. 3 for comparison. It is clear from the figure that in CuCl, $Z_{1,2}$ and Z_3 exciton bands appear as high and low energy bands

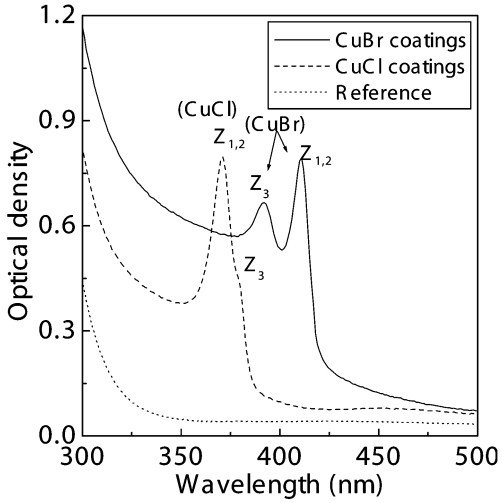

Fig. 3 A comparison of the exciton absorption of CuCl and CuBr nanocrystals at room temperature.

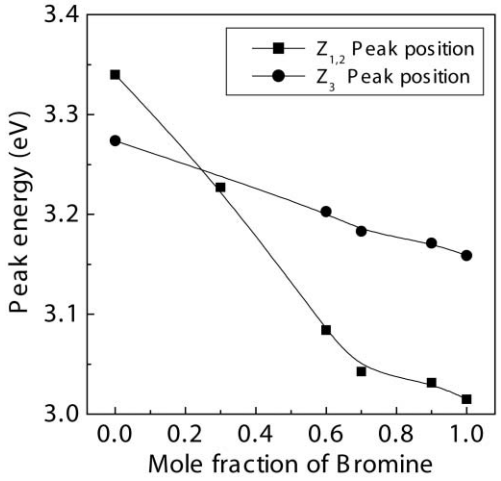

Fig. 4 Energies of the $Z_{1,2}$ and Z_3 absorption peaks in $CuCl_xBr_{1-x}$ as a function of bromide concentration $(1 - x)$ at 25 °C.

respectively. On the other hand in CuBr their positions are reversed (*i.e.* $Z_{1,2}$ and Z_3 bands correspond to the low and high energy bands respectively).

To understand this reverse behavior of CuCl and CuBr, Cardona[20] suggested that the top of the valence band (Γ_{15}) is triply degenerate without spin orbit splitting in the zincblende structure. This degeneracy is reduced by spin orbit splitting to doubly degenerate (Γ_8) and singlet (Γ_6) states. The Γ_8 doublet state gives a $Z_{1,2}$ peak whereas the Γ_6 state gives the Z_3 peak. Since the strongest line should be the doublet line because of the larger number of states available for transition from the doubly degenerate valence band, they concluded that the spin orbit splitting is negative in the case of CuCl, *i.e.* the triplet in CuCl is inverted. The energies of the $Z_{1,2}$ and Z_3 absorption peaks of $CuCl_xBr_{1-x}$ (x = 0–1) at 25 °C are shown as a function of bromide ion concentration $(1 - x)$ in Table 1.

The $Z_{1,2}$ and Z_3 absorption peak positions of the thin films containing $CuCl_xBr_{1-x}$ (x = 1–0) as the function of the bromide ion concentration $(1 - x)$ at 25 °C are plotted in Fig. 4. The variation of the absorption peak energy is in good agreement with that obtained by Cardona.[20] From this figure it is clear that the two curves cross each other at $x = 0.24$; this indicates that there is no spin orbit splitting at this concentration. The band width of the Z_3 exciton band increases appreciably as the concentration $(1 - x)$ exceeds 0.24, and the band appears on the high energy side of the $Z_{1,2}$ exciton. This fact is interpreted in terms of the shorter life time of the higher energy Z_3 exciton owing to the scattering into the lower state of the $Z_{1,2}$ exciton.[21] When the Z_3 exciton is lower in energy than that of the $Z_{1,2}$ exciton, there is no state for the Z_3 exciton to be scattered to except within its own band, and the life time of the excitons is longer. Thus the Z_3 exciton band is sharper. At $x = 0.24$ the relative position of the two bands are inverted but the separation between them is not too large, the $Z_{1,2}$ band is much weaker than the Z_3 band. The intensity of the $Z_{1,2}$ band increases gradually as $(1 - x)$ increases from 0.24 and the separation between Z_3 and the $Z_{1,2}$ bands increases.

Table 1 The $Z_{1,2}$ and Z_3 peak positions of $CuCl_xBr_{1-x}$ at 25 °C as a function of bromide ion concentration $(1 - x)$

$(1 - x)$ in $CuCl_xBr_{1-x}$	$Z_{1,2}$ Peak position/eV	Z_3 Peak position/eV
0	3.34	3.27
0.3	3.22	—
0.6	3.08	3.20
0.7	3.04	3.18
0.9	3.03	3.17
1.0	3.02	3.16

Temperature dependence of CuBr exciton peaks

In the case of CuCl, the positions of the $Z_{1,2}$ and Z_3 excitons has been found by Kaifu and Komatsu[22] to be dependent on the temperature. This has not been reported for CuBr and therefore the temperature dependence of the $Z_{1,2}$ and Z_3 excitons in CuBr was studied. The absorption spectra of CuBr nanoparticles are shown in Fig. 5 at different temperatures. The absorption spectra were recorded in the spectral range from 300–1000 nm (*i.e.* 4.13–1.24 eV) at four different temperatures. However the spectra shown here are only in the range from 2.5–3.5 eV. The positions of the absorption maxima for Z_3 and $Z_{1,2}$ are plotted in Fig. 6a as a function of temperature. These figures indicate that the splitting of the $Z_{1,2}$ and Z_3 excitons remains practically constant as the temperature changes. The same observations were made by Garro *et al.*[23] in the case of the CuCl nanoparticles.

The dependence of the excitons of CuCl on temperature has been explained by Garro *et al.*[23] by postulating that the vibration of the Cu^+ ions leads to an increase in the energy gap while the opposite is true for the halogen ions. They considered that the copper vibrates predominantly at low frequencies, while Cl vibrates mainly at high frequencies, because of its smaller mass. Hence the Cu vibrations cause a linear variation of the energy gap at rather low temperatures. Hence the

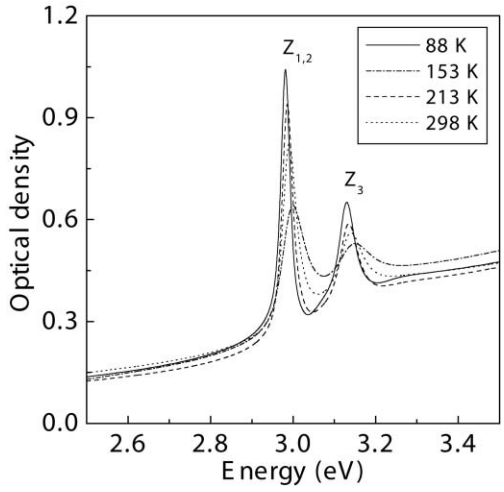

Fig. 5 Variation in the exciton peaks of thin films containing CuBr nanocrystals at different temperatures.

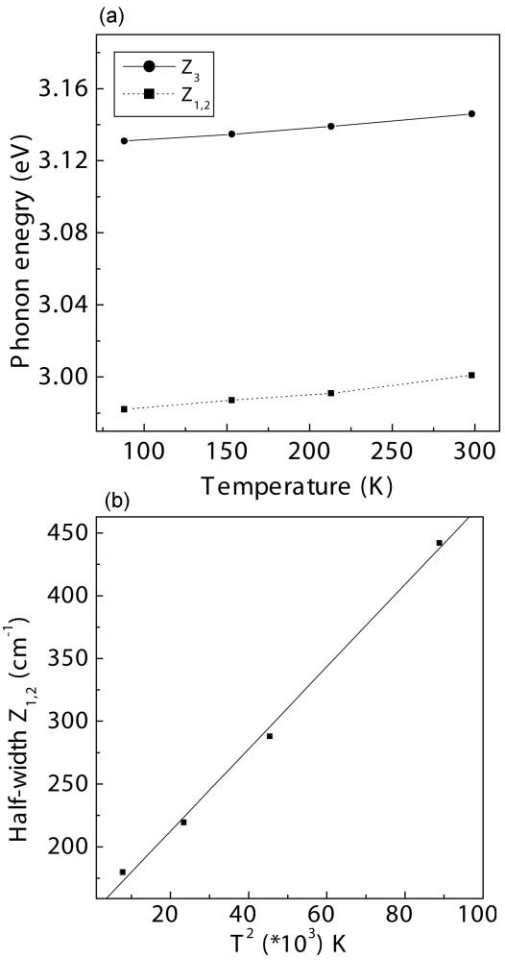

Fig. 6 (a) Z_3 and $Z_{1,2}$ absorption peak positions as a function of temperature. (b) Half-width of the $Z_{1,2}$ exciton peak as a function of the square of the temperature.

analogous temperature dependence observed in the case of CuBr can also be interpreted in similar way.

The half-widths of the $Z_{1,2}$ exciton peak are plotted in Fig. 6b as a function of T^2. It can be seen that the data points lie in a straight line. All the plots are limited to the temperatures below 298 K, because at higher temperatures the determination of the width is uncertain. Here only the $Z_{1,2}$ line is considered, because Z_3 is superimposed on higher order exciton or satellite lines,[24] and therefore it's half-width varies in a more complicated way. To determine the half-width of the $Z_{1,2}$ peak, the spectrum was deconvoluted, and the curve fitted on the lower energy peak (*i.e.* the $Z_{1,2}$ peak) was used for half-width calculations.

The broadening of the peak with temperature has been explained by Toyazawa's theory,[25] who found that the half-width, in terms of the energy units, can be expressed as $W = g^2(kT)^2/8\pi^2\, m^*u^2$, where K is Boltzmann's constant, m^* is the reduced effective mass of the exciton, u is the longitudinal sound velocity and g is the dimensionless coupling constant. This equation implies that the half-width of the excitons is proportional to T^2.

XRD analysis: substitution of Cl^- by Br^- ions

The sequential substitution of Cl^- by Br^- was also followed by XRD analysis. Fig. 7 shows the XRD patterns of the films containing varying amounts of bromide and chloride. When there is no HBr in the solution all three diffraction peaks of CuCl (Fig. 7a) were obtained. The addition of 5.50×10^{-3} to 1.65×10^{-2} mole HBr per 4.2×10^{-3} mole Cu_2O dissolved in

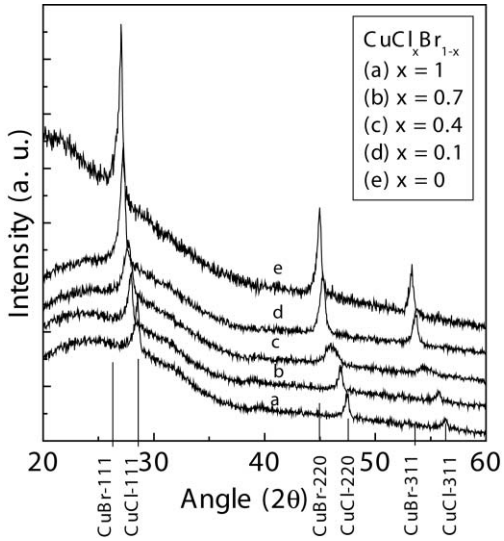

Fig. 7 X- ray diffraction patterns of thin films containing $CuCl_xBr_{1-x}$: (a) $x = 1$, (b) $x = 0.7$, (c) $x = 0.4$, (d) $x = 0.1$, (e) $x = 0$.

8.2×10^{-2} mole HCl gradually shifts the peaks toward lower 2θ's. Addition of 1.85×10^{-2} mole HBr finally leads to all three characteristic peaks (Fig. 7e) of CuBr.

In order to see if Br^- ions are sequentially substituting Cl^- ions or whether they are occupying the interstitial voids for the intermediate compositions, Lattice parameters of the compounds $CuCl_xBr_{1-x}$ ($x = 0$–1) were determined from the XRD spectra using the following relation

$$\frac{1}{d^2} = \frac{h^2+k^2+l^2}{a^2},$$

where, h, k, l are Miller indices, d is the interplaner spacing and a is the lattice constant.

Precise lattice constants were determined by taking an average of the lattice constant based on three peaks (111), (220) and (311). For the samples without HBr, a lattice constant of 5.42 Å was determined which is in agreement with the literature-cited value for CuCl.[26] Addition of HBr gradually increases the lattice constant and finally gives a value of 5.68 Å, for 1.85×10^{-2} mole HBr, which is in good agreement with the literature reported value for CuBr.[26] On plotting the lattice constants as a function of bromide ion concentration a straight line was obtained, which indicates that the chloride ions are substituted by the bromide ions in the complete composition range thus confirming Vegard's law.[27]

Scherrer's equation,[28] which correlates the width of the diffraction peak at half maximum β and the Bragg diffraction angle, can be used to determine the diameter (d) of the copper halide particles in these thin films. The β value was taken from the recorded XRD patterns for the most intense (111) peak and the crystallite diameters were calculated to be 11, 11.5, 7.0, 9.0 and 12 nm for the $CuCl_xBr_{1-x}$ particles having $x = 1$, 0.7, 0.4, 0.1 and 0 respectively.

In order to see the shape and size of the particles formed in thin films, high-resolution transmission electron microscopic (HR-TEM) analysis was carried out. Fig. 8 shows the HR-TEM micrograph of the sample containing $CuCl_xBr_{1-x}$ (for $x = 0.7$) nanoparticles. This figure shows the formation of nanometer sized spherical particles having a diameter ranging from 5–15 nm. The range in particle size observed here is good agreement with that calculated using the Scherrer formula.

Conclusions

The sol–gel process has successfully been used for the synthesis of nanocomposite thin films containing $CuCl_xBr_{1-x}$ ($x = 1$–0)

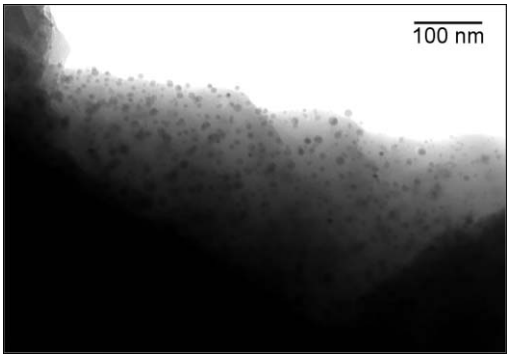

Fig. 8 HR-TEM image of the thin film containing $CuCl_xBr_{1-x}$ (x = 0.7) nanoparticles.

nanocrystals. Copper could be stabilized in the Cu^+ state as an acid soluble halocuprate complex in solution in the presence of acetonitrile. Stepwise substitution of chloride ions by bromide ions was carried out successfully. For the samples having no bromide, UV-VIS absorption spectrum showed a sharp absorption edge at 371 nm. Addition of HBr shifted the peak towards a higher wavelength and characteristic peaks corresponding to $CuCl_xBr_{1-x}$ were observed. Addition of 1.85×10^{-2} mole HBr finally produced peaks at 391 and 411 nm corresponding to CuBr indicating the complete substitution of chloride by bromide ions. These experiments confirmed that the position of the absorption edge can favorably be shifted by the substitution of chloride ions by bromide ions. The XRD technique also supported these observations very well.

However, further research has to be conducted in order to find a dense matrix that prohibits the oxidation of cuprous to cupric ions, thus opening the field to applications in, for example, UV-VIS filters with sharp edges and non-linear optics.

Acknowledgements

The authors wish to thank Dr U. Werner for carrying out the TEM measurements and the State of Saarland, Germany, for financial support.

References

1 L. E. Brus, *Appl. Phys., A: Solid Surf.*, 1992, **53**, 465–474.
2 P. Gillot, J. C. Merle, R. Levy, M. Robino and B. Hönerlage, *Appl. Phys., B: Photophys. Laser Chem.*, 1991, **153**, 403.
3 R. K. Jain and R. C. Lind, *J. Opt. Soc. Am.*, 1983, **73**(5), 647.
4 Y. Kayamura, *Phys. Rev. B*, 1988, **38**, 9797.
5 A. I. Efros and A. A. Efros, *Sov. Phys. Semicon.*, 1982, **16**, 772.
6 A. I. Ekimov and A. A. Onushchenko, *JETP Lett.*, 1989, **40**, 1136.
7 N. Sugimoto, M. Yamamoto, T. Manabe and S. Ito, in *Proceedings of the International Conference on New Glasses*, Tokyo, 16–17 October, 1991.
8 M. Nogami, Y. Q. Zhu, Y. Tohyama and K. Nogasaka, *J. Am. Ceram. Soc.*, 1991, **74**(1), 238.
9 M. Nogami, Y. Q. Zhu and K. Nagasaka, *J. Non-Cryst. Solids*, 1991, **134**, 71.
10 T. Takada, T. Yano, A. Yasumori, M. Yamane and J. D. Mackenzie, in *Proceedings of the 32nd Glass & Photonics Materials Meeting* Osaka, 26–29 November, 1999, p. 67.
11 M. Nogami, K. Ozaki, K. Nagasaka and A. Nakamura, *Proc. 37th Spring Meeting Jpn. Appl. Phys.*, 1990, 31a-N-1.
12 Corning Glasses, No. 2403 to 2434 and 3480 to 3486.
13 Schott Glasses, No. RG : 610 to RG 715 and OG 5515 to OG 5590.
14 G. Suyal, M. Mennig and H. Schmidt, *J. Non-Cryst. Solids*, 2002, in press.
15 D. G. Peters and R. L. Caldwell, *Inorg. Chem.*, 1967, **6**, 1478.
16 F. A. Cotton and G. Wilkinson, *Advanced Inorganic Chemistry*, Wiley, NewYork, 3rd edn., 1971, p. 906.
17 J. A. Ruller, G. M. Williams and E. L. Friebele, *Ceram. Trans.*, 1992, **28**, 499.
18 B. N. Figgies, *Introduction to Ligand Field*, Wiley, New York, 1966, p. 306.
19 J. D. Lee, *Concise Inorganic Chemistry*, Chapman and Hall, London, 1996, p. 825.
20 M. Cardona, *Phys. Rev.*, 1963, **129**(1), 69.
21 I. Toyozawa, *J. Phys. Chem. Solids*, 1964, **25**, 59.
22 Y. Kaifu and T. Komatsu, *Phys. Status Solidi B*, 1971, **48**, K125.
23 N. Garro, A. Cantarero, M. Cardona, T. Ruf, A. Göbet, C. Lin, K. Reimann, S. Rübenacke and M. Steube, *Solid State Commun.*, 1996, **98**(1), 27.
24 J. Ringeissen, A. Coret and S. Nikitine, *Localized Excitations in Solids*, Plenum Press, New York, 1968, p. 297.
25 Y. Toyozawa, *Progr. Theor. Phys.*, 1962, **27**, 89.
26 L. Börnstein, *Numerical Data and Fundamental Relationship in Science and Technology, II-VI Compounds*, New Series III 17b, ed. O. Madelung, Springer Verlag, Berlin, 1982.
27 M. Yashima, N. Ishizawa and M. Yoshimura, *J. Am. Ceram. Soc.*, 1992, **75**(6), 1550.
28 B. E. Warren, *X-Ray Diffraction*, Addison-Wesley, Reading, MA, 1969, p. 253.